IEEE Access
Multidisciplinary | Rapid Review | Open Access Journal

Received July 27, 2021, accepted August 18, 2021, date of publication August 23, 2021, date of current version August 27, 2021.

Digital Object Identifier 10.1109/ACCESS.2021.3106671

A DOA Estimation Method for Uniform Circular Array Based on Virtual Interpolation and Subarray Rotation

TAO LIANG[1,2,3], MIN ZHU[1,3], AND FENG PAN[4]

[1]Ocean Acoustic Technology Center, Institute of Acoustics, Chinese Academy of Sciences, Beijing 100190, China
[2]University of Chinese Academy of Sciences, Beijing 100190, China
[3]Beijing Engineering Technology Research Center of Ocean Acoustic Equipment, Beijing 100190, China
[4]Institute of Information Engineering, Chinese Academy of Sciences, Beijing 100093, China

Corresponding author: Min Zhu (zhumin@mail.ioa.ac.cn)

This work was supported in part by the National Key Research and Development Program of China under Grant 2016YFC0300300.

ABSTRACT A uniform linear array (ULA) or a multi-element planar array composed of uniform linear arrays is the main applied research array for direction-of-arrival (DOA) estimation in array signal processing. In recent years, the uniform circular array (UCA) is getting more attention because of its consistent azimuthal beam resolution, but the DOA estimation algorithm of a UCA is complex and difficult to implement. To solve this problem, a UCA positioning method based on virtual interpolation and subarray rotation (VISAR) is proposed. This method effectively reduces the computational complexity of DOA estimation for a UCA, and the simulation analysis of the algorithm shows that in terms of positioning performance, the proposed algorithm is better than the existing virtual interpolation algorithms in the case of a low signal-to-noise ratio (SNR).

INDEX TERMS Direction of arrival (DOA), uniform circular array (UCA), virtual Interpolation, subarray rotation.

I. INTRODUCTION

In array signal processing, if the manifold of the array satisfies the form of a Vandermonde matrix, such as a uniform linear array (ULA) [1], [2], an L-shaped array [3]–[5] or a multivariate planar array composed of uniform linear arrays [6], [7], then classical eigenvalue decomposition methods, such as multiple signal classification (MUSIC) [8] or estimating signal parameter via rotational invariance techniques (ESPRIT) [9], can be used to estimate the direction of arrival. However, the effective aperture of linear array changes with the azimuth, so the azimuthal beam width of these arrays is inconsistent.

Because the manifold matrix of a uniform circular array is not a Vandermonde matrix, the eigenvalue decomposition method cannot be directly used to find the direction. But as a special array antenna in array signal processing, due to the symmetry it possesses, a UCA can scan a beam azimuthally through 360° with little change in the beam width. Ioannides [10] compares the UCA with a uniform rectangular array (URA) in the context of adaptive beamforming and draws the conclusion that the azimuth measurement accuracy is higher than that of a planar array composed of ULAs. Thus, beamforming methods can be used for precise azimuthal estimation of a UCA, such as minimum variance distortion-less response (MVDR) [11]. However, when there is a deviation between the supposed and true direction vectors, there will be a sharp decline in the performance of the traditional MVDR algorithm, and accurate results cannot be obtained. Phase mode excitation beamforming is a more widely used beamforming algorithm for UCAs. Divas and Gibson [12] presents this beamforming method in detail and demonstrates the practical example of beam space radiation pattern synthesis. Askari clarifies the conclusion in [13] that when array sensors are directional and the optimum beamformer is deployed, the sector transformed beamformer has better performance than the ordinary transformed one. Although a UCA has better azimuth resolution, in consideration of the beam width limitation, it is difficult for a UCA to obtain accurate positioning results just by using a beamforming algorithm.

Mathews and Zoltowski [14], [15] proposes a method combining phase excitation beamforming and Bessel function

The associate editor coordinating the review of this manuscript and approving it for publication was Ananya Sen Gupta.

transformation to transform the manifold of a UCA to a form in which eigenvalue decomposition can be used to estimate the DOA. Further research on this algorithm has been performed. Belloni and Koivunen [16] analyzes the error of this algorithm, provides design guidelines for choosing the key UCA configuration parameters and proposes a novel technique for bias removal. Xu *et al.* [17] proposes an accurate and reliable technique to estimate DOA of source signals based on random sample consensus algorithm. Wang *et al.* [18] studies the performance of the algorithm in the case of coherent sources. Pesavento and Bohme [19] decouples the azimuth estimation from the elevation parameter to obtain a better positioning result in a search-free procedure when the elements are directional. Li and Chen [20] improves the resolution performance under a low SNR by introducing a phase shift matrix before weight vectors to rebuild a conjugate symmetric beam space steering vector in the process of phase mode excitation. In addition to the above, Lian and Zhou [21] uses the propagator method to estimate DOA in beam space for UCA. Because the method does not use eigen-decomposition, it can reduce the computational load significantly. Pan and Zhou [22] proposed a method for UCA based on the manifold separation technique and propagator method, this algorithm provides close to Cramer-Rao bound performance even under the limitation of the element's number. These methods can obtain accurate positioning results, but the high algorithm complexity and large transformation error in the calculation process make them hard to implement.

Sometimes the virtual interpolation technique can be applied for formation transformation if the formation of an array does not satisfy the DOA estimation algorithm requirements. The array interpolation method is first proposed by Bronez [23], and there are some improved algorithms [24]–[26]. Most of these kinds of methods can be directly used in arbitrary arrays [27]. For a linear array, Zhou transforms a coprime array to a ULA by virtual interpolation and reconstructs the Toeplitz covariance matrix for DOA estimation with an increased number of degrees of freedom by minimizing the atomic norm of a virtual measurement vector in a gridless manner [28]–[30]. Qin *et al.* [31] fills the holes in a sparse array to form a ULA by shifting the physical array by half the wavelength along its axis. The virtual interpolation technique can also be applied to a UCA for DOA estimation. Sun proposes an algorithm for a UCA in [32], called the twice virtual interpolation algorithm (TVIA). This method uses virtual interpolation twice to obtain two virtual arrays, and there is a rotation invariant factor between the virtual arrays and original array. The elevation angle can be calculated by one-dimensional ESPRIT and substituted into the real array manifold to search the azimuth angle by one-dimensional MUSIC. This method is much simpler, but the elevation and azimuth angles cannot be estimated in pairs and one-dimensional search is still needed, which leads to high computation and storage costs. Based on this method, Xu *et al.* [33] proposes a method termed multi-direction virtual array transformation algorithm (MVATA), which constructs two multi-direction virtual arrays to obtain the rotation invariant factor between the virtual arrays and actual array. The DOA estimation can be performed by one-time ESPRIT. The elevation and azimuth angles are obtained in pairs, and there is no need to use MUSIC to search the spectrum; thus, the computations and costs can be distinctly reduced compared with TVIA.

In this paper, a DOA estimation algorithm for a UCA based on virtual interpolation and subarray rotation (VISAR) is proposed. The algorithm symmetrically divides a UCA into two groups of subarrays along the X-axis and Y-axis. It uses the subarrays rotated 180° about the virtually interpolated reference elements and the nonrotated subarrays to form a new rotation invariant array for which ESPRIT can be used to estimate the DOA. Compared with TVIA and MVATA, the algorithm has lower computational complexity in the interpolation process, and the single target positioning performance of the algorithm is better than that of TVIA and MVATA under the low SNR incoherent noise environment.

II. SIGNAL MODEL AND TVIA AND MVATA APPROACHES

A. SIGNAL MODEL

As shown in Figure 1, in the Cartesian coordinate system, a UCA array composed of N elements is on the $X-Y$ plane. The radius of the circle is r, and the origin of the coordinate system coincides with the center of the array. A single narrowband sound source emitted from the far field impinges on the array.

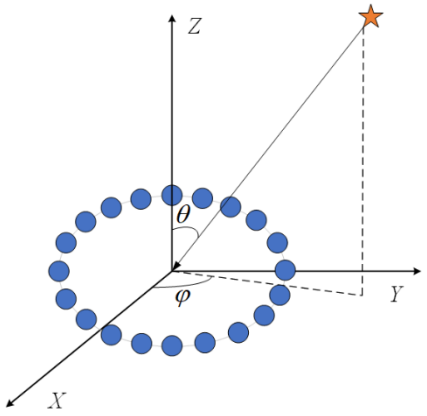

FIGURE 1. Uniform circular array signal receiving model.

The received signal can be expressed as

$$\boldsymbol{X}(t) = \boldsymbol{A}S(t) + \boldsymbol{N}(t) \tag{1}$$

$S(t)$ is the sound source, $N(t)$ is the additive noise vector of $1 \times N$, obeying the Gaussian distribution $(0, \sigma^2)$, and the manifold can be expressed as

$$\boldsymbol{A} = \left[e^{j\xi\cos(\varphi-\gamma_1)}, \ldots, e^{j\xi\cos(\varphi-\gamma_m)}\right]^T \tag{2}$$

where $\xi_i = \frac{2\pi r}{\lambda}\sin\theta_i$ and $\gamma_m = \frac{2\pi m}{N}$, $m = 1, 2, \ldots, N$.

The steering matrix expressed in the above formula is not a Vandermonde matrix, so DOA estimation cannot be directly conducted by using the classical eigenvalue decomposition methods.

B. TVIA AND MVATA ALGORITHMS

According to [29] and [30], TVIA and MVATA both construct two virtual arrays that have rotational invariance with the original arrays through virtual interpolation, and DOA estimation is performed on the whole array formed by the original array and virtual arrays via eigen-decomposition.

In the interpolation process, the two algorithms divide the area near the target into several sectors and calculate the array manifolds of the original array and virtual arrays in the sectors. Then, the relationship between these arrays can be obtained. The following is a brief introduction of interpolation algorithm in [30].

Assume the elevation and azimuth of the target are in $\boldsymbol{\Theta}_\theta \in [\theta_l, \theta_m]$ and $\boldsymbol{\Theta}_\varphi \in [\varphi_l, \varphi_m]$, respectively, and $\Delta\gamma$ is the interpolation step. Thus, $\boldsymbol{\Theta}_\theta$ and $\boldsymbol{\Theta}_\varphi$ can be discretized as

$$\boldsymbol{\Theta}_\theta = \{\theta_x = \theta_l + (x-1)\Delta\gamma | 1 < x < X, \theta_x < \theta_m\} \quad (3)$$
$$\boldsymbol{\Theta}_\varphi = \{\varphi_y = \varphi_l + (y-1)\Delta\gamma | 1 < y < Y, \varphi_y < \varphi_m\} \quad (4)$$

The manifold of the original array $\boldsymbol{A}_f$ can be presented as

$$\boldsymbol{A}_f = [\cdots \boldsymbol{A}(\theta_x, \varphi_y) \cdots], \quad \theta_x \in \Theta_\theta, \ \varphi_y \in \Theta_\varphi \quad (5)$$

$\boldsymbol{A}'$ and $\boldsymbol{A}''$ are the manifolds of the two virtual arrays. Suppose that there are relationships $\boldsymbol{B}'$ and $\boldsymbol{B}''$ such that

$$\boldsymbol{A}_f' = \boldsymbol{B}_{k1}^H \cdot \boldsymbol{A}_f \quad (6)$$
$$\boldsymbol{A}_f'' = \boldsymbol{B}_{k2}^H \cdot \boldsymbol{A}_f \quad (7)$$

$\boldsymbol{B}'$ and $\boldsymbol{B}''$ are calculated by the singular value decomposition method. With the singular value decomposition of $\boldsymbol{A}_f$, the following can be obtained:

$$\boldsymbol{A}_f = \boldsymbol{U}[\sum, 0][\boldsymbol{V}_1, \boldsymbol{V}_2]^H \quad (8)$$

where $\boldsymbol{U}$ is the $N \times N$ left singular matrix, $\sum$ is the $N \times N$ singular value matrix, $[\boldsymbol{V}_1, \boldsymbol{V}_2]^T$ is the $W \times W$ right singular matrix, and the size of matrix $\boldsymbol{V}_1$ is $W \times N$. Combined with (6), (7), and (8), the relationships $\boldsymbol{B}'$ and $\boldsymbol{B}''$ can be obtained.

$$\boldsymbol{B}' = \boldsymbol{U}\sum^{-1}\boldsymbol{V}_1^H(\boldsymbol{A}_f')^H \quad (9)$$
$$\boldsymbol{B}'' = \boldsymbol{U}\sum^{-1}\boldsymbol{V}_1^H(\boldsymbol{A}_f'')^H \quad (10)$$

Then, the signal received by the virtual arrays can be calculated by using the signal received by the original array and the relationships $\boldsymbol{B}'$ and $\boldsymbol{B}''$. Finally, according to the rotational invariance between the virtual arrays and the original array, the ESPRIT algorithm is used to estimate the DOA.

The interpolation process of the TVIA algorithm is only performed along the vertical axis, as shown in Figure 2. After calculating the elevation by using the ESPRIT algorithm, TVIA uses MUSIC to search the azimuth. Different from TVIA, the virtual arrays of the MVATA algorithm and the original array have a deviation angle in the elevation direction, as shown in Figure 3. Therefore, the MVATA algorithm using the ESPRIT algorithm can obtain the elevation and azimuth angles in pairs. These two methods have many advantages, but the interpolation process requires considerable computation and has errors.

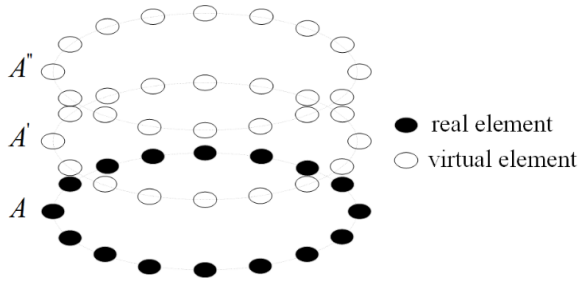

FIGURE 2. Array configuration of TVIA.

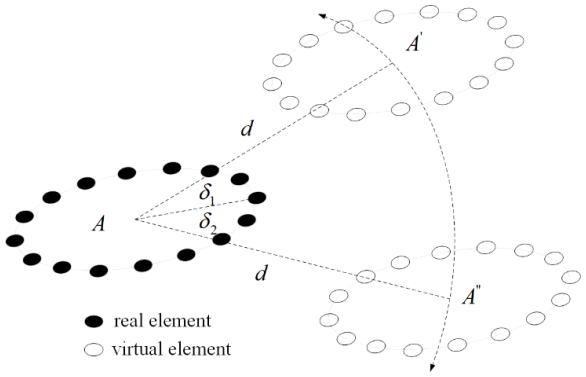

FIGURE 3. Array configuration of MVATA.

III. PRINCIPLE OF THE PROPOSED ALGORITHM

According to the central symmetry and even number of elements of a UCA, the relationship of the coordinate angle between the elements is

$$\gamma_{N/2+m} = \gamma_m + \pi, \ m = 1, 2, \ldots, N/2 \quad (11)$$

Expressed by a trigonometric function, this becomes

$$\cos(\varphi - \gamma_{N/2+m}) = -\cos(\varphi - \gamma_m) \quad (12)$$

It is easy to know that the centrosymmetric elements in the array manifold are conjugate to each other. Therefore, the manifold of the array can be divided into two parts, and the corresponding circular array is also divided into two symmetric subarrays.

$$\boldsymbol{A} = [\boldsymbol{b}(\theta, \varphi), \boldsymbol{c}(\theta, \varphi)]^T \quad (13)$$

where

$$\boldsymbol{b}(\theta, \varphi) = [e^{j\xi\cos(\varphi-\gamma_1)}, \ldots, e^{j\xi\cos(\varphi-\gamma_{N/2})}] \quad (14)$$
$$\boldsymbol{c}(\theta, \varphi) = \left[e^{j\xi\cos(\varphi-\gamma_{N/2+1})}, \ldots, e^{j\xi\cos(\varphi-\gamma_N)}\right] = \left[e^{-j\xi\cos(\varphi-\gamma_1)}, \ldots, e^{-j\xi\cos(\varphi-\gamma_{N/2})}\right] \quad (15)$$

The corresponding elements in $\boldsymbol{c}(\theta, \varphi)$ and $\boldsymbol{b}(\theta, \varphi)$ are conjugate to each other.

Let the subarray with steering vector $\boldsymbol{c}(\theta, \varphi)$ be rotated 180° about the coordinate origin. At this time, the rotated subarray coincides with the subarray with steering vector $\boldsymbol{b}(\theta, \varphi)$, and the received signal phases of the corresponding elements are consistent between these two subarrays. If other reference points are used as the center of rotation, then the distance between the corresponding elements of the two subarrays will be consistent, and it is easy to know that the phase difference will be the same.

Considering the problem of array segmentation, assumed that the received signal is a narrowband far-field signal, the normalized vector of the target direction is $\overrightarrow{\boldsymbol{TO}}(X, Y, Z)$, the coordinates of the origin are $O(0, 0, 0)$, and the coordinates of actual elements are $P_i(x_i, y_i, 0), i = 1, 2, \ldots, 12$. According to the normalized vector $\overrightarrow{\boldsymbol{TO}}$ and the element vector $\overrightarrow{\boldsymbol{P_iO}}$, the phase difference ϕ_i of the received signal between actual element P_i and origin coordinates O can be calculated. Knowing that $\left|\overrightarrow{\boldsymbol{P_iO}}\right|$ is the distance between element P_i and origin O, which is equal to the radius of the array r, and the normalized distance $\left|\overrightarrow{\boldsymbol{TO}}\right|$ is equal to 1, phase difference ϕ_i can be expressed as

$$\begin{aligned}\phi_i &= -\frac{2\pi r}{\lambda} \cdot \frac{\overrightarrow{\boldsymbol{P_iO}} \cdot \overrightarrow{\boldsymbol{TO}}}{\left|\overrightarrow{\boldsymbol{P_iO}}\right| \cdot \left|\overrightarrow{\boldsymbol{TO}}\right|} = -\frac{2\pi}{\lambda} \cdot \frac{\overrightarrow{\boldsymbol{P_iO}} \cdot \overrightarrow{\boldsymbol{TO}}}{\left|\overrightarrow{\boldsymbol{TO}}\right|} \\ &= -\frac{2\pi}{\lambda} \cdot (x_i \cdot X + y_i \cdot Y) = \phi_{xi} + \phi_{yi} \end{aligned} \tag{16}$$

ϕ_i can be divided into the X-axis phase difference ϕ_{xi} and Y-axis phase difference ϕ_{yi} according to the above formula. Therefore, the array can be divided along the X-axis and Y-axis.

Based on the above discussion, the UCA is divided into four subarrays along the X-axis and Y-axis directions. If there are elements on the X-axis or Y-axis, these elements are shared by the subarrays that have been divided. The virtual elements V_{x1} and V_{x2} are set up along the positive half of the X-axis, and the virtual elements V_{y1} and V_{y2} are set up along the positive half of the Y-axis. Inserting two elements on the axis just satisfies with the conditions for the ESPRIT algorithm after subarray rotation, and the computation is minimal. The distance between virtual elements is set to d, as shown in Figure 4. The subarray on the positive half of the X-axis is rotated 180° about V_{x1} and V_{x2}, and the subarray on the positive half of the Y-axis is rotated 180° about V_{y1} and V_{y2}. The distance between the subarrays after rotation is consistent and set to D. It is easy to know that $D = 2d$. To prevent the grating lobes, D should be less than $\lambda/2$, so d is less than $\lambda/4$.

Suppose that there is a UCA with N elements, and there is no element on the axes. Let's take dividing the array along the X-axis as an example, as shown in Figure 5. $\boldsymbol{A}_{x1}$ is the subarray on the negative half of the X-axis after the division, and $\boldsymbol{A}_{x2}$ is the subarray on the positive half of the X-axis that needs to be rotated. The virtual elements V_{x1} and V_{x2} have been interpolated along the X-axis. On the X-Y plane, the coordinates of the virtual elements V_{x1} and V_{x2} are expressed as $P_{v_{x1}}(x_{v_{x1}}, y_{v_{x1}}, 0)$ and $P_{v_{x2}}(x_{v_{x2}}, y_{v_{x2}}, 0)$.

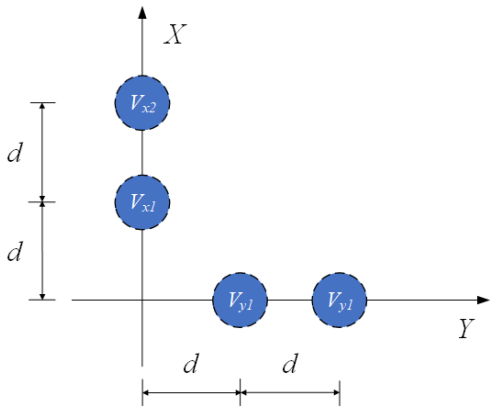

FIGURE 4. Virtual interpolation diagram.

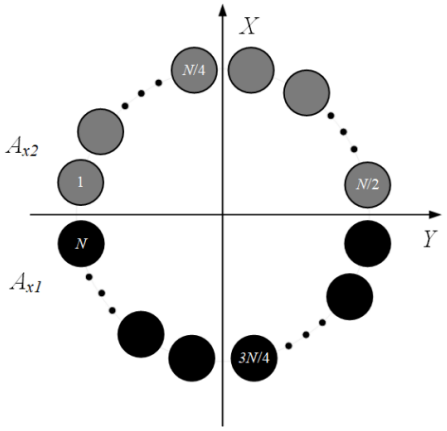

FIGURE 5. Diagram of segmentation along the X-axis array.

First, consider the rotation of subarray A_{x2} about virtual element V_{x1}. The actual coordinates of subarray A_{x2} are $P_i(x_i, y_i, 0), i = 1, 2, \ldots, N/2$, and the coordinates of the elements after rotation by 180° are $P_i'(x_i', y_i', 0)$. The coordinate rotation formula can be expressed as

$$\begin{bmatrix} x_i' \\ y_i' \\ z_i' \end{bmatrix} = \boldsymbol{R} \begin{bmatrix} x_i - x_{v_1} \\ y_i - y_{v_1} \\ 0 \end{bmatrix} + \begin{bmatrix} x_{v_1} \\ y_{v_1} \\ 0 \end{bmatrix} \tag{17}$$

where, $\boldsymbol{R}$ is the rotation factor.

$$\boldsymbol{R} = \begin{bmatrix} \cos(-180°) & \sin(-180°) & 0 \\ -\sin(-180°) & \cos(-180°) & 0 \\ 0 & 0 & 1 \end{bmatrix} \tag{18}$$

In combination with (16), after the rotation about the virtual element V_{x1}, the phase difference ϕ_{x_2}' becomes

$$\begin{aligned}\phi_{x2}' &= -\frac{2\pi}{\lambda} \cdot (x_i' X + y_i' Y) \\ &= -\frac{2\pi}{\lambda} \cdot \left[(2 \cdot x_{v_1} - x_i) \cdot X + (2 \cdot y_{v_1} - y_i) \cdot Y\right] \\ &= 2\phi_{v_{x1}} - \phi_{x2} \end{aligned} \tag{19}$$

Similarly, when the subarray is rotated about the virtual element V_{x2}, the phase difference ϕ''_{x2} becomes

$$\phi''_{x2} = 2\phi_{v_{x2}} - \phi_{x2} \tag{20}$$

It can be seen from (14) and (15), that the elements of the positive half axis guidance vector and negative half axis guidance vector are conjugate to each other, and the relationship of the phase differences relative to the origin between the corresponding elements is $\phi_{x_2} = -\phi_{x_1}$. Therefore, the phase difference $\Delta\phi$ between the elements of the rotated subarray and the corresponding elements of the nonrotated subarray is linearly related to the phase of the center of rotation $P_{v_{xi}}$.

The phase information of virtual elements in the X-axis direction can be expressed as

$$\Delta\phi_x = \frac{2\pi d}{\lambda}\sin\theta\cos\varphi \tag{21}$$

In the Y-axis direction, it can be expressed as

$$\Delta\phi_y = \frac{2\pi d}{\lambda}\sin\theta\sin\varphi \tag{22}$$

The array rotated about the X-axis is shown in Figure 6.

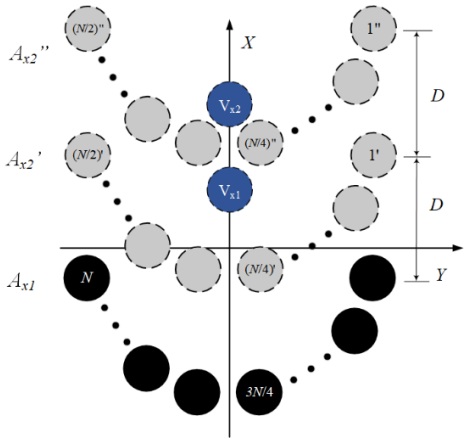

FIGURE 6. Diagram of VISAR along X-axis.

According to (21) and (22), when r, d, λ, and γ_m are known, $\Delta\phi_x$ and $\Delta\phi_y$ can be deduced from the received signal of any two elements in the array. Thus, the manifold of the whole array can be expressed as

$$\boldsymbol{A}'_x = \begin{bmatrix} e^{j\beta_{N/2+1}} & e^{j\beta_{N/2+2}} & \cdots & e^{j\beta_N} \\ e^{j(\beta_{N/2+1}+\Delta\phi_x)} & e^{j(\beta_{N/2+2}+\Delta\phi_x)} & \cdots & e^{j(\beta_N+\Delta\phi_x)} \\ e^{j(\beta_{N/2+1}+2\cdot\Delta\phi_x)} & e^{j(\beta_{N/2+2}+2\cdot\Delta\phi_x)} & \cdots & e^{j(\beta_N+2\cdot\Delta\phi_x)} \end{bmatrix}^T \tag{23}$$

The matrix above satisfies the form of a Vandermonde matrix, where,

$$\beta_i = \xi\cos(\varphi - \gamma_i), \quad i = N/2+1, N/2+2, \ldots, N \tag{24}$$

It can be concluded that there is rotational invariance between the virtual subarray and the nonrotated subarray after virtual interpolation along and subarray rotation about the X-axis, and the ESPRIT algorithm can be used for X-axis direction DOA estimation. Similarly, the same result can be obtained after virtual interpolation along and subarray rotation about the Y-axis.

In the VISAR process, the phase information of the signal received by the virtual elements, namely, (21) and (22), needs to be computed. When there is a single target, the signal received by any element in the UCA can be expressed as

$$y(t) = s(t)e^{j\frac{2\pi r}{\lambda}\sin\theta(\cos\varphi\cos\gamma_m+\sin\varphi\sin\gamma_m)} + n_m(t) \tag{25}$$

Because the virtual elements are set up along the coordinate axis, the received signal of virtual elements can be easily calculated based on the received signal of any two actual elements. However, when multiple targets exist, every element in the array receives signals from multiple targets at different times. Suppose there are K targets and (25) becomes

$$y(t) = s(t)\sum_{k=1}^{K} e^{j\frac{2\pi r}{\lambda}\sin\theta_k(\cos\varphi_k\cos\gamma_m+\sin\varphi_k\sin\gamma_m)} + n_m(t) \tag{26}$$

There are multiple angle variables of different targets, and the received signal of virtual elements cannot be obtained from the received signal of any two actual elements. Hence, the algorithm proposed by this paper is only applicable to a single target.

According to (25), an element will introduce noise $n_m(t)$ when receive the signal. Since the computation of the phase information of the virtual elements needs to use the signals received by any two actual elements, there is an error in the phase information of virtual elements. However, it has little effect; if the noise $n_m(t)$ is irrelevant, such as white Gaussian noise.

IV. IMPLEMENTATION STEPS

1) The uniform circular array is divided into two groups of symmetric subarrays along the X-axis and Y-axis, half of which are nonrotated subarrays and the other half of which are rotated subarrays.
2) Four virtual elements are interpolated along the X and Y half axes as the rotation reference points.
3) After the rotation of subarrays about the reference points, virtual subarrays are formed along the X-axis and Y-axis.
4) Two new arrays are formed by the virtual subarrays and nonrotated subarrays along the X-axis direction and Y-axis direction. There is rotational invariance within the two new arrays. ESPRIT can be used to estimate the direction on the X-axis and Y-axis.

V. COMPUTATIONAL COMPLEXITY ANALYSIS

In this section, the computational complexity of the proposed algorithm is compared with that of TVIA and MVATA. Assume that the element number of the uniform circular array is N and the number of snapshots is M. The computational complexity of the algorithm is shown in Table 1.

TABLE 1. Comparison of computational complexity.

Algorithm	Multiplication	Addition
$A = U[\Sigma, 0][V_1\ V_2]^H$	$N^3 + 2N^2$	$(N^2+2)(N-1)$
$B = U\Sigma^{-1}V_1^H(A')^H$	$2(N^3 + 2N^2K)$	$2N(N-1)(N+K) + 2N^2(K-1)$
total	$3N^3 + (2K+1)N^2$	$3N^3 + (4K-5)N^2 + 2(1-K)N - 2$
TVIA		
total	$8N^3 + 4(M+5+2L_1)N^2 + 2(1-L_1)N + 3$	$8N^3 + 4(M+2L_1)N^2 + 2(2-3L_1)N - 6$
MVATA		
total	$8N^3 + 6(M+2)N^2 + 2N + 17$	$8N^3 + (5M-8)N^2 + (6-M)N - 4$
VISAR		
total	$\frac{27}{8}N^3 + 9(\frac{1}{4}M+1)N^2 + 2(2M+1)N + 8M + 6$	$\frac{27}{8}N^3 - \frac{9}{4}(M-2)N^2 + 5N - 6$

In [26], computational complexity analysis of TVIA and MVATA is carried out, and that of MVATA is obviously less than that of TVIA. However, this paper does not give the computational complexity of linear virtual interpolation. Before the comparison, the computational complexity of virtual interpolation needs to be added.

Suppose that in the MVATA algorithm, the space near the target is divided into $K = 100$ cones, and this value is substituted into the corresponding formula in Table 1. Figure 7 and Figure 8 show the variation curves of the variation in the difference between the total multiplications and total additions of MVATA and VISAR with the number of array elements N and snapshots M. It can be found from the figures that the differences between the total multiplications and the total additions are always greater than 0. Therefore, it can be concluded that the computational complexity of the VISAR algorithm proposed in this paper is much less than that of the TVIA algorithm and MVATA algorithm.

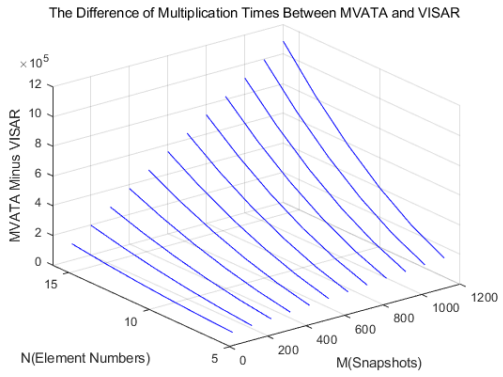

FIGURE 7. Comparison diagram of multiplication.

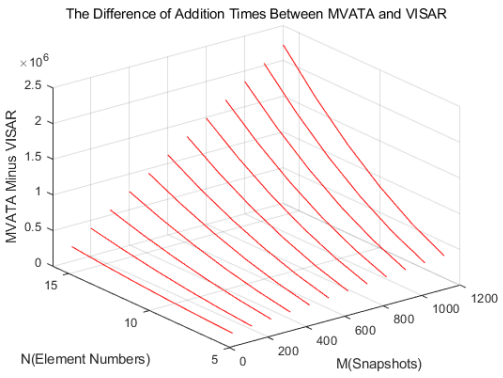

FIGURE 8. Comparison diagram of addition.

VI. SIMULATION ANALYSIS

In this section, three experiments are presented to show the characteristics of the proposed VISAR algorithm and the performance improvement compared with TVIA and MVATA in the single target case. A UCA of radius $r = \lambda$ with 12 elements is employed, where λ is the wavelength. Virtual elements are located on the half-axes d and $2d$ from the origin, and the search step size of TVIA and MVATA is set to 0.1° in the comparison experiment. Assume that a narrowband signal impinges on the array and the elevation and azimuth of the target are 15° and 10°. The noise is spatially and temporally white Gaussian incoherent noise. SNR is the ratio of the received signal power to noise power, and the unit is dB in the experiments.

A. EXPERIMENT 1

Suppose that the snapshot number is 500. After 500 Monte Carlo simulations, the positioning result diagram of the proposed algorithm when the SNR is 10 dB is shown in Figure 9.

The figure shows that the results tightly converge near the real position of the target. Hence, the VISAR algorithm can accurately position the target.

B. EXPERIMENT 2

To obtain the relationship between the algorithm performance and distance d between the virtual elements and the origin, the root-mean-square errors (RMSEs) of VISAR when

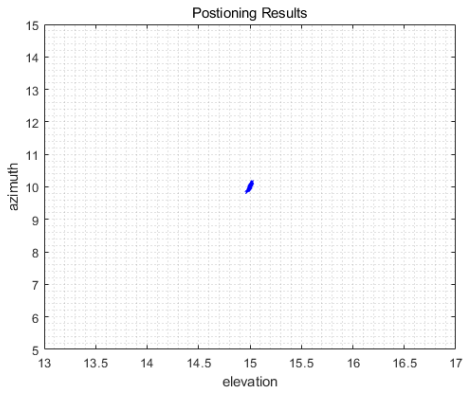

FIGURE 9. Positioning results of VISAR.

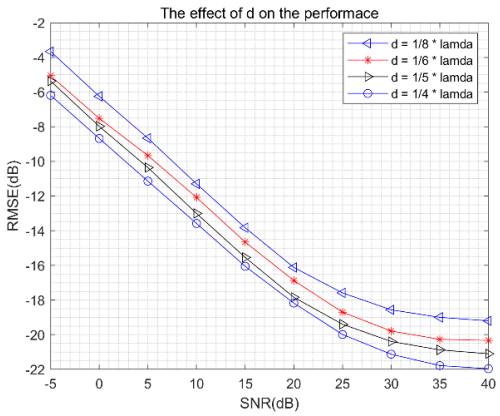

FIGURE 10. The effect of d on the performance of VISAR.

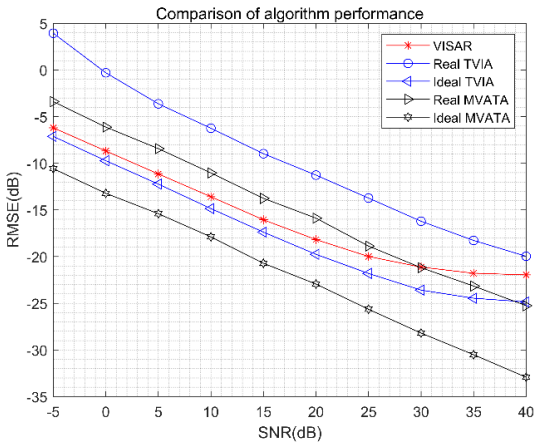

FIGURE 11. Comparison of algorithm performance.

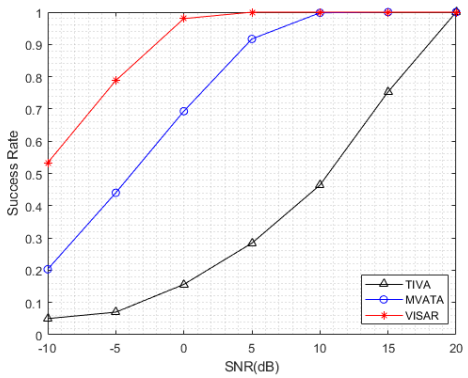

FIGURE 12. Comparison of estimated success rat.

d takes different values are compared. From the above, it is known that d cannot be larger than $\lambda/4$, so we take d equal to $\lambda/8$, $\lambda/6$, $\lambda/5$ and $\lambda/4$ as examples to compare the RMSEs.

The RMSE is calculated according to the formula

$$RMSE = \sqrt{\frac{1}{T}\sum_{t=1}^{T}(\hat{\theta}-\theta)^2 + (\hat{\varphi}-\varphi)^2} \tag{27}$$

where, T is the Monte Carlo simulation number, set to 500. $\hat{\theta}$ and $\hat{\varphi}$ are the estimated elevation and azimuth, θ and φ are the true elevation and azimuth.

Assume that the elevation and azimuth between the target and origin are 20° and 30°, the snapshot number is 400, and the Monte Carlo number is 500. When d is less than $\lambda/4$, with increasing d, the array length becomes larger. Understandably, the phase sensitivity of the whole array is also increased, as shown in Figure 10, and the positioning performance improves.

C. EXPERIMENT 3

The RMSEs of the positioning results are calculated to compare the positioning performances of TVIA, MVATA and VISAR.

Assume that the interpolation region of the azimuth is [5°, 15°] and the interpolation region of the elevation is [10°, 25°]. Virtual elements of VISAR are set at $\frac{\lambda}{4}$ and $\frac{\lambda}{2}$ on the X-axis and Y-axis, respectively, so the distance between the subarrays after rotation is $\frac{\lambda}{2}$. The snapshot number is 400. Figure 11 shows the positioning performance when the SNR is $-5dB \sim 40dB$. 'Ideal TVIA' and 'Ideal MVATA' are the performance curves of TVIA and MVATA when virtual arrays exist.

Figure.12 shows the comparison of the estimated success rate between VISAR, TVIA and MVATA. In the TVIA algorithm and MVATA algorithm, the interpolation regions of the azimuth and elevation are still defined as [5°, 15°] and [10°, 20°]. Since the assumed azimuth and elevation of the target are 10° and 15°, the correct azimuth and elevation angles are estimated to be those within ±0.05° of the actual values. The range of SNR is $-10dB \sim 20dB$.

It can be seen from the figures that in the case of a low SNR, the performance of the VISAR algorithm is significantly better than that of MVATA and TVIA in the single target case.

VII. CONCLUSION

To reduce the computational complexity of the uniform circular array positioning algorithm, this paper proposes a uniform circular array positioning algorithm based on virtual interpolation and subarray rotation. The array is symmetrically divided into two groups of subarrays along the X-axis and Y-axis, the subarrays are rotated about the virtual

interpolation elements to form new arrays with the nonrotated subarrays, and ESPRIT is used to calculate the positioning results in the end. By comparison with TVIA and MVATA, it can be concluded that the VISAR algorithm proposed in this paper has lower computational complexity, and its single target positioning performance is better than that of TVIA and MVATA under the low SNR incoherent noise enviroment.

REFERENCES

[1] L. Aihua, X. Zhang, Q. Yang, and W. Deng, "Fast DOA estimation algorithms for sparse uniform linear array with multiple integer frequencies," *IEEE Access*, vol. 6, pp. 29952–29965, May 2018.

[2] Z. Ye and X. Xu, "DOA estimation by exploiting the symmetric configuration of uniform linear array," *IEEE Trans. Antennas Propag.*, vol. 55, no. 12, pp. 3716–3720, Dec. 2007.

[3] Y. Hua, T. K. Sarkar, and D. D. Weiner, "An L-shaped array for estimating 2-D directions of wave arrival," *IEEE Trans. Antennas Propag.*, vol. 39, no. 2, pp. 143–146, Feb. 1991.

[4] N. Tayem and H. M. Kwon, "L-shape 2-dimensional arrival angle estimation with propagator method," *IEEE Trans. Antennas Propag.*, vol. 53, no. 5, pp. 1622–1630, May 2005.

[5] N. Tayem, K. Majeed, and A. A. Hussain, "Two-dimensional DOA estimation using cross-correlation matrix with L-shaped array," *IEEE Antennas Wireless Propag. Lett.*, vol. 15, pp. 1077–1080, Dec. 2016.

[6] Y. Wu, G. Liao, and H.-C. So, "A fast algorithm for 2-D direction-of-arrival estimation," *Signal Process.*, vol. 83, no. 8, pp. 1827–1831, 2003.

[7] P. Heidenreich, A. M. Zoubir, and M. Rubsamen, "Joint 2-D DOA estimation and phase calibration for uniform rectangular arrays," *IEEE Trans. Signal Process.*, vol. 60, no. 9, pp. 4683–4693, Sep. 2012.

[8] R. O. Schmidt, "Multiple emitter location and signal parameter estimation," *IEEE Trans. Antennas Propag.*, vol. AP-34, no. 3, pp. 276–280, Mar. 1986.

[9] R. Roy and T. Kailath, "Esprit-estimation of signal parameters via rotational invariance techniques," *IEEE Trans. Acoust., Speech, Signal Process.*, vol. 37, no. 7, pp. 984–995, Jul. 1989.

[10] P. Ioannides and C. A. Balanis, "Uniform circular and rectangular arrays for adaptive beamforming applications," *IEEE Antennas Wireless Propag. Lett.*, vol. 4, pp. 351–354, 2005.

[11] M. Askari and M. Karimi, "Quadratically constrained beamforming applied to UCA," in *Proc. 20th ICEE*, Tehran, Iran, 2012, pp. 1178–1183.

[12] J. G. Davis and A. A. P. Gibson, "Phase mode excitation in beamforming arrays," in *Proc. Eur. Radar Conf.*, Manchester, U.K., Sep. 2006, pp. 1786–1789.

[13] M. Askari and M. Karimi, "Sector beamforming with uniform circular array antennas using phase mode transformation," in *Proc. 21st Iranian Conf. Electr. Eng. (ICEE)*, Mashhad, Iran, May 2013, pp. 1–6.

[14] C. P. Mathews and M. D. Zoltowski, "Eigenstructure techniques for 2-D angle estimation with uniform circular arrays," *IEEE Trans. Signal Process.*, vol. 42, no. 9, pp. 2395–2407, Sep. 1994.

[15] C. P. Mathews and M. D. Zoltowski, "Performance analysis of the UCA-ESPRIT algorithm for circular ring arrays," *IEEE Trans. Signal Process.*, vol. 42, no. 9, pp. 2535–2539, Sep. 1994.

[16] F. Belloni and V. Koivunen, "Beamspace transform for UCA: Error analysis and bias reduction," *IEEE Trans. Signal Process.*, vol. 54, no. 8, pp. 3078–3089, Aug. 2006.

[17] Z. Xu, S. Wu, Z. Yu, and X. Guang, "A robust direction of arrival estimation method for uniform circular array," *Sensors*, vol. 19, no. 20, p. 4427, Oct. 2019.

[18] J. Wang, X. Gu, and Y. Liu, "The coherent DOA estimation of uniform circular array based on SVD algorithm," in *Proc. Int. Conf. Electr. Control Eng.*, Yichang, China, Sep. 2011, pp. 6147–6151.

[19] M. Pesavento and J. F. Bohme, "Direction of arrival estimation in uniform circular arrays composed of directional elements," in *Proc. Sensor Array Multichannel Signal Process. Workshop*, Rosslyn, VA, USA, 2002, pp. 503–507.

[20] S. Li and H. Chen, "A novel method of DOA estimation on sparse uniform circular array," in *Proc. CIE Int. Conf. Radar (RADAR)*, Guangzhou, China, Oct. 2016, pp. 1–4.

[21] X. Lian and J. Zhou, "2-D DOA estimation for uniform circular arrays with PM," in *Proc. 7th Int. Symp. Antennas, Propag. EM Theory*, Oct. 2006, pp. 1–4.

[22] J. Pan and J. Zhou, "Beamspace PM-root-MUSIC for uniform circular array based on MST," in *Proc. Int. Joint Conf. Comput. Sci. Optim.*, Apr. 2009, pp. 899–901.

[23] T. P. Bronez, "Sector interpolation of non-uniform arrays for efficient high-resolution bearing estimation," in *Proc. Int. Conf. Acoust., Speech, Signal Process. (ICASSP)*, New York, NY, USA, vol. 5, 1988, pp. 2885–2888.

[24] B. Friedlander, "Direction finding using an interpolated array," in *Proc. Int. Conf. Acoust., Speech, Signal Process.*, Albuquerque, NM, USA, vol. 5, Apr. 1990, pp. 2951–2954.

[25] B. Friedlander and A. J. Weiss, "Direction finding for wideband signals using an interpolated array," in *Proc. 25th Asilomar Conf. Signals, Syst. Comput.*, Pacific Grove, CA, USA, vol. 1, 1991, pp. 583–587.

[26] Q. Li, Y. Jiang, and X. Diao, "A DOA estimation algorithm of virtual array based on beam forming," in *Proc. Int. Conf. Electr. Control Eng.*, Yichang, China, Sep. 2011, pp. 945–948.

[27] P. Yang, F. Yang, Z.-P. Nie, B. Li, and X. Tang, "Robust adaptive beamformer using interpolation technique for conformal antenna array," *Prog. Electromagn. Res. B*, vol. 23, pp. 215–228, Jan. 2010.

[28] C. Zhou, Y. Gu, X. Fan, Z. Shi, G. Mao, and Y. D. Zhang, "Direction-of-arrival estimation for coprime array via virtual array interpolation," *IEEE Trans. Signal Process.*, vol. 66, no. 22, pp. 5956–5971, Nov. 2018.

[29] C. Zhou, Y. Gu, Z. Shi, and Y. D. Zhang, "Off-grid direction-of-arrival estimation using coprime array interpolation," *IEEE Signal Process. Lett.*, vol. 25, no. 11, pp. 1710–1714, Nov. 2018.

[30] Z. Chen, C. Fan, and X. Huang, "Interpolation-based direction-of-arrival estimation for coprime arrays via covariance matrix fitting," *IEEE Access*, vol. 8, pp. 149133–149141, 2020.

[31] G. Qin, M. G. Amin, and Y. D. Zhang, "DOA estimation exploiting sparse array motions," *IEEE Trans. Signal Process.*, vol. 67, no. 11, pp. 3013–3027, Jun. 2019.

[32] X.-J. Sun, G.-Y. Zhang, B. Tang, and Q. Gan, "Circle array receiving signal 2D-DOA separable estimation based on twice virtual interpolations," *J. Electron. Inf. Technol.*, vol. 30, no. 8, pp. 1890–1892, Mar. 2011.

[33] K.-J. Xu, W.-K. Nie, D.-Z. Feng, X.-J. Chen, and D.-Y. Fang, "A multi-direction virtual array transformation algorithm for 2D DOA estimation," *Signal Process.*, vol. 125, pp. 122–133, Aug. 2016.

TAO LIANG received the B.S. degree from Zhengzhou University, Zhengzhou, China, in 2013, and the M.S. degree from Beijing Institute of Technology, Beijing, China, in 2015. He is currently pursuing the Ph.D. degree with the Institute of Acoustics, Chinese Academy of Sciences, Beijing. His research interests include underwater acoustic communication and array signal processing.

MIN ZHU received the B.S. degree from the University of Science and Technology of China, Hefei, China, in 1994, and the M.S. and Ph.D. degrees from the Graduate University of Chinese Academy of Sciences, Beijing, China, in 2001 and 2006, respectively. He is currently a Professor with the Institute of Acoustics, Chinese Academy of Sciences. He is one of the second batches of leading scientists for the 10,000 Talents Project. His research interests include underwater acoustic communication and networks, acoustic doppler velocimetry technology, underwater acoustic detection, and acoustic systems of underwater human-occupied vehicles.

FENG PAN received the B.S. degree from Beijing Union University, Beijing, China, in 1985. He is currently a Researcher with the Institute of Information Engineering, Chinese Academy of Sciences. His research interest includes underwater acoustic system research and implementation. He is a fellow of the Acoustical Society of China.